IEEE Open Access Journal of
Power and Energy

Received 18 December 2023; revised 19 June 2024; accepted 29 July 2024.
Date of publication 5 August 2024; date of current version 16 August 2024.

Digital Object Identifier 10.1109/OAJPE.2024.3438153

Fast Fault-Tolerant Grid Frequency Measurement

CHRIS WEMBRIDGE[1,2] (Member, IEEE), MARK DAVIES[2], JAMES LORD[2], EVAN FRANKLIN[1] (Member, IEEE), SARAH LYDEN[1] (Member, IEEE), AND MICHAEL NEGNEVITSKY[1] (Fellow, IEEE)

[1]School of Engineering, University of Tasmania, Hobart, TAS 7001, Australia
[2]TasNetworks, Hobart, TAS 7009, Australia

CORRESPONDING AUTHOR: C. WEMBRIDGE (chris.wembridge@tasnetworks.com.au)

The work was supported by TasNetworks and the Australian Research Council Industrial Transformation Training Centre in Energy Technologies for Future Grids under Contract IC210100021.

ABSTRACT As power systems adopt greater levels of asynchronous generation, operators increasingly need to accurately monitor and manage their systems. With inverter-based generation progressively displacing traditional synchronous generators, power systems generally experience increased rate of change of grid frequency and wider propagation of voltage disturbances after a network contingency event. Inverter-based resources are now being leveraged to mitigate larger frequency disturbances, by delivering fast frequency control ancillary services. For this to be effective, accurate and robust, fast and fault-tolerant grid frequency measurements are needed. Commonly deployed frequency measurement techniques are susceptible to significant measurement error when exposed to unbalanced faults and frequency deviations. More robust techniques for measuring frequency are thus needed. This paper describes in detail a measurement strategy that extracts the continuous phase angle of the positive phase sequence phasor, from voltage signals. The method is demonstrated to provide robust measurements in the presence of simultaneously and rapidly varying voltage and frequency. From real-world measurements, using the Tasmanian power system as a case-study, the method is shown to be equivalent to or outperform measurement devices currently deployed in power systems. This paper provides all necessary control block diagrams required for integration into various modelling packages and frequency measurement devices.

INDEX TERMS Fast frequency response, fault-tolerant, frequency control ancillary services, grid frequency measurement, inverter-based resources, positive sequence phasor, ROCOF.

NOMENCLATURE

IBR	Inverter-based Resources.
PMU	Phasor Measurement Unit.
FCAS	Frequency Control Ancillary Services.
NEM	National Electricity Market.
ROCOF	Rate-of-Change-of-Frequency.
ZCD	Zero-crossing Detection.
PLL	Phase Locked Loop.
FFT	Fast Fourier Transform.
PSP	Positive Sequence Phasor.
VT	Voltage Transformer.
NREL	National Renewable Energy Laboratory.
SMIB	Single Machine Infinite Bus.
HVDC	High Voltage Direct Current.
AEMO	Australian Energy Market Operator.
EMT	Electro-magnetic Transient.
PPS	Positive Phase Sequence.
ZPS	Zero Phase Sequence.
MAF	Moving Average Filter.
RRL	Resistor-Resistor//Inductor (source impedance).
SLG	Single-line to Ground.
DLG	Double-line to Ground.
3*LG*	Three-line to Ground.
L-L	Line to Line.

I. INTRODUCTION

POWER system operators globally have been preparing for the increased adoption of inverter-based resources (IBR) by connecting phasor measurement units (PMU) to their key network nodes. PMUs allow operators to routinely download and store the time-synchronized measurements

following major events. One critical function of PMUs is the measurement of system frequency. Frequency is generally calculated from fundamental voltage or current measurements through proprietary algorithms. The algorithms used, and hence the resultant frequency measurement, can vary significantly between different manufacturers and devices. Some calculation methods are particularly intolerant to the combination of frequency and voltage deviation which occurs during and immediately after the occurrence of unbalanced faults. This can result in measurement error and variability [1], [2], [3].

As the generation mix in power systems shifts from high-inertia synchronous generation to inverter-based resources, system operations and markets are evolving in order to manage the faster frequency excursions that occur as a result.

For example, a new 'very fast' Frequency Control Ancillary Services (FCAS) market was introduced recently in the Australian National Electricity Market (NEM), targeting an active power response within 1 second in the presence of a Rate of Change of Frequency (ROCOF) of $\pm$ 1 Hz/s (or $\pm$ 2 Hz/s in the case of the Tasmanian power system, which is electrically connected to but not synchronized with the rest of the NEM) [4]. This change recognizes that ROCOF will increase in power systems in future [5], [6], [7] and provides a new market mechanism to help bound that increase. For this very fast service to be successful, it is critical that the frequency measurements used by the participating automatic control systems are reliable and fault-tolerant.

Frequency deviations that are significant enough to warrant a response from an automatic control system or the attention of power system operators are predominantly driven by system faults [8]. The profile of voltage waveforms can change dramatically during fault events. Thus, the accurate measurement of grid frequency is exposed to the greatest challenge when the measurement source is in close electrical proximity to faults [9]. However, the effect of faults propagate more widely in 'weak' networks [10]. As synchronous generation is increasingly replaced by IBR, 'weak' networks will become prevalent. Grid frequency measurements will thus become more challenging across the network in future. Any measurement of grid frequency which is required for practical purposes must continue to produce accurate results, even under conditions where system strength is low.

Accurate grid frequency measurement is not a new challenge in the power industry, with many authors tackling the problem using various techniques [1], [7], [15], [16]. Authors have highlighted that careful tuning of measurement algorithms is needed [5], [14], while considering the trade-off between fast response time and error suppression [8], [11], [12]. Judicious engineering decisions are required to design a control system that can accurately track grid frequency under various system conditions, during fault and frequency events [8], and in weak grids and low inertia systems [12], [14]. For fast measurement in strong systems with high-inertia, simple methods may represent a suitable solution [9], [15]. However, with the development of IBR dominated power systems, it is necessary to use techniques that are both fast and fault-tolerant [6], [12], [13], [14], [15], [16].

Zero-crossing detection (ZCD) is a common grid frequency measurement method. It is based on the measurement of time differences between zero-crossings of the voltage waveforms [17]. ZCD methods are prone to producing large measurement errors during network faults, since they are susceptible to phase angle jumps, harmonic voltage distortion, and multiple zero-crossings and "DC" voltage offsets that may occur during faults [18]. In particular, phase angle jumps, which are a natural consequence of most faults, can alter the time difference between voltage zero-crossings by up to $\pm$ 33% [19]. This results in considerable challenges for conventional frequency measurement techniques [20].

Phase-locked loop (PLL) based algorithms are commonly used by inverter-based resources for converter control [7]. However, similar to the performance of ZCD methods, they can suffer from poor performance in the presence of phase jumps and distortion [9]. Another common approach for frequency measurement is to use Fast Fourier Transform (FFT) based algorithms. Discrete Fourier Transforms in particular offer a relatively low computational requirement for frequency estimation, especially when determining the fundamental frequency component only [7], [16]. Similar to the ZCD method, for power systems where high ROCOF, phase jumps and distortion regularly occur during and after network faults and disturbances, measurements produced via FFT based methods are prone to error [9], [12], [20].

While the application of post-processing treatments, such as smoothing or incorporating frequency rate limits, can mask some of these errors, the overall final measurement often embeds an inaccuracy, due to the fault, that is unrepresentative of the underlying grid frequency. The ZCD, PLL and FFT methods reach fundamental design constraints when aiming for a grid frequency measurement with high rate of change of frequency (ROCOF) capability.

Early work by Phadke et al. has paved the way for reliable grid frequency measurement: their techniques are mathematically described in [21]. Their work highlighted the problems of measuring time difference based on zero-crossings, and instead used the continuous phase angle embedded within the complete sinusoidal waveforms. The positive sequence phasor (PSP) method which we describe in this work preserves these original principles, while providing an implementation that is compatible with the computing power of modern PMUs. While all network VT based grid frequency measurements require control limits and filters, the PSP method described herein requires less filtering, which creates a wider bandwidth grid frequency measurement for the same level of reliability.

An extensive literature review has been presented by researchers at MIT and NREL, comparing the performance of six of the top performing and readily available frequency measurement algorithms [9]. While the authors present detailed comparisons via side-by-side simulations,

they conclude that there is a need for research to extend the comparison to include real-world data measured by utilities from troublesome transient events. In this work, the following has been presented:

1. We extend the comparison of methods to include actual PMU measurements, obtained by devices currently deployed in a large power system.
2. We address the current gap in the literature by providing fully detailed block diagrams for a fast, fault-tolerant PSP method,
3. Further implementation of this method has been conducted in software to assess measurement accuracy under weak grid conditions alongside other commonly deployed measurement methods.
4. We have described a method that can be readily implemented in software packages or on hardware and can be readily tuned to meet a given user's grid conditions and grid requirements.

The remainder of the paper is structured as follows: an assessment of frequency measurements produced by several in-service PMUs, during a known fault event in a real power system, is presented in section II; in section III the block diagram implementation of the PSP method used in this paper is provided, and its ability to reliably extract the continuous phase angle of the positive phase sequence phasor from three phase network voltage signals is described; in section IV this PSP method is type-tested with voltage and frequency disturbances using a simplified Single Machine Infinite Bus (SMIB) system, is benchmarked against actual PMU measurements from the Tasmanian power system after a severe network fault, and is also compared with a simple FFT, PLL and ZCD methods with identical filtering; a brief summary and outlook on the applicability of the PSP method in power systems is provided in section V.

II. ASSESSMENT OF REAL-WORLD FREQUENCY MEASUREMENTS

A key contribution of this paper is to evaluate the effectiveness and reliability of frequency measurements currently performed in practical power systems, and to benchmark both existing techniques and the method proposed in this paper under challenging real-world transient conditions. To achieve this we use high-resolution data, collected from a power system typified by high penetration of non-synchronous generation, during an observed severe transient event. The Tasmanian power system is used as a case study, owing to its susceptibility to larger frequency and voltage excursions during and after network events.

The Tasmanian system is connected via a monopolar HVDC interconnector to the remainder of the Australian NEM and has a power demand in the range of 800 to 1700 MW. The Tasmanian power system can be characterised as a "light" power system, with relatively low levels of inertia and system strength: the dominant energy resources in the system are hydro-generation units (2200 MW capacity), but these are distant from major load centres, and wind generation (568 MW capacity) plus HVDC (480 MW import capacity) results in the system being often dominated by IBR. These characteristics make Tasmania a suitable case study to demonstrate future power systems, where the impacts of poor grid frequency measurement are more obviously apparent and can have larger impact.

The outputs of three PMUs during a fault event are assessed. These consist of three different manufactured products, each connected at the same location in the Tasmanian power system, within a large substation.

Fig. 1 shows the frequency measurement produced by each PMU during a severe multiple fault event that occurred on 14th October 2022. The series of events originated with the double circuit line trip of a critical tie line in the central network of the Tasmanian power system. An operating incident report was prepared by AEMO, detailing the sequence of incident events [22]. The traces highlight the wide variability in PMU measurement: PMU 'A' and 'B' show marked divergences from the underlying grid system frequency.

TABLE 1. Parameters of the control block diagram in Fig. 3.

Symbol	Description	Value
V_{base}	Base voltage RMS L-G	Per project
f_o	Nominal frequency	50 or 60 Hz
ω_o	Band-pass angular frequency	$2\pi f_o$ (rad/s)
ζ	Band-pass damping ratio	0.707
Vhi_hys	Hysteresis voltage high threshold	0.10 pu
Vlo_hys	Hysteresis voltage low threshold	0.05 pu
T_i	Integrator time constant	80 ms
T_d	Processing time step delay	Delta-T
F_max	Maximum frequency	55 or 66 Hz
F_min	Minimum frequency	45 or 54 Hz
df/dt_max	Maximum ROCOF	5 Hz/s
df_lim	Change of frequency limit	0.5 Hz
T_f	Net delay of filter blocks (Fig. 3(A)(B)	20 ms

III. IMPLEMENTATION OF THE PROPOSED POSITIVE SEQUENCE PHASOR MEASUREMENT METHOD

For the representation of the PSP measurement method, a high-level overview is provided in Fig. 2. The complete block diagram is also provided in Fig. 3. This level of detail enables its implementation in both PMU type hardware or EMT simulation environments. The control system parameters are listed in Table 1 and have been tuned to track a ROCOF of up to ± 5 Hz/s, as required for compliance of IBRs [23].

The PSP benefits from two fundamental improvements, (1) the filtering is computationally more efficient to implement as it only requires filtering to produce 90° rotations, whereas 120° rotations are more common for other transformations, (2) the PSP uses its own frequency measurement output to

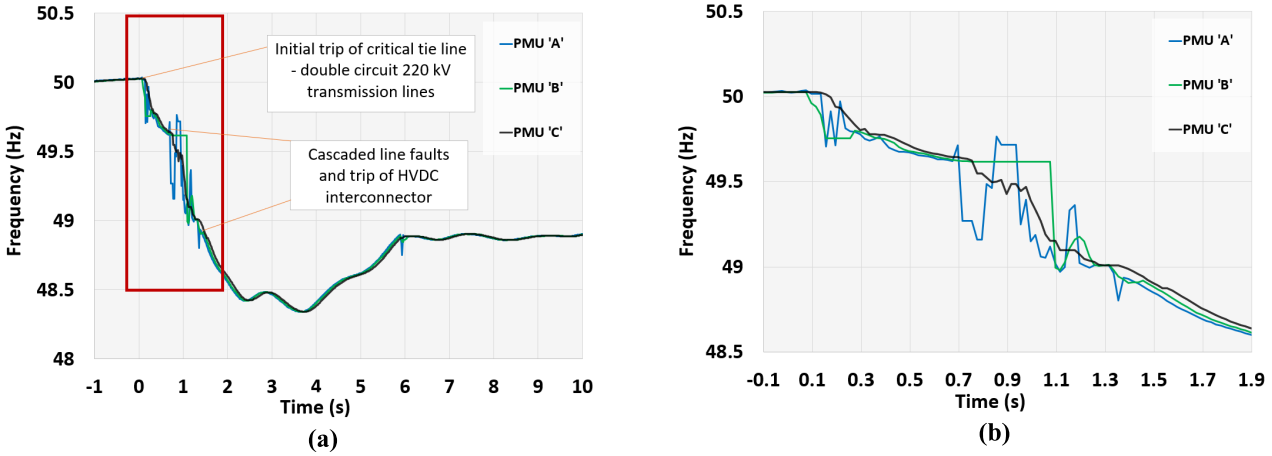

FIGURE 1. **(a) PMU frequency traces from a fault event in the Tasmanian power system, (b) zoomed-in PMU frequency traces.**

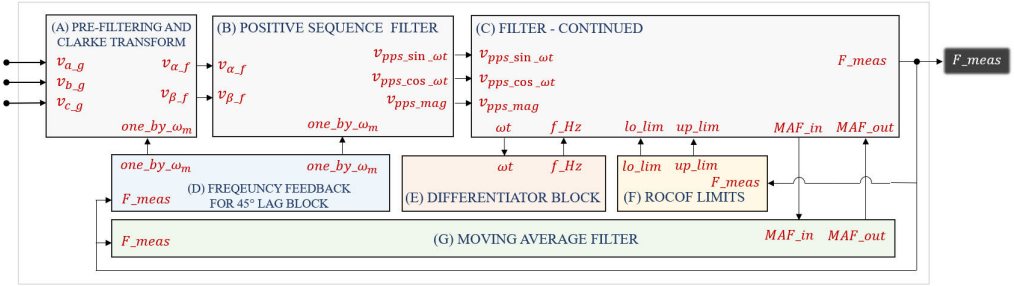

FIGURE 2. **High level block diagram for the PSP method.**

lock the 90° lag delay, which is an elegant way to maintain the rotational accuracy as frequency moves away from nominal.

(A) Pre-filtering and Clarke Transformation: The inputs to the PSP frequency measurement method are three single phase-ground VT signals, which are converted to the orthogonal Clarke (α, β) quantities as shown in Fig. 3(A) [24]. The input filters are anti-alias band pass filters centred on the fundamental frequency. The unwanted zero phase sequence (zps) components are removed before the Clarke transformation. Two cascaded first-order lag blocks provide additional filtering.

(B) Positive Sequence Filter: the method for extracting sine and cosine terms in positive phase sequence (pps) is shown in Fig. 3(B). For accurate rejection of the negative phase sequence components, over a wide range of power frequencies, the lag blocks must retain the net 90° phase shift.

(C) Positive Sequence Filter – continued: The phase of the pps voltage, ωt, is conventionally extracted as shown in Fig. 3(C), noting that ωt appears in the form of a sawtooth (ramp) waveform.

(D) Frequency Feedback for 45° Lag Block: This is achieved by locking their time constants to the measured fundamental frequency; refer to Fig. 3(D), where the frequency feedback for the 45° lag blocks is produced.

(E) Differentiator Block: The frequency output, f_Hz, is then calculated by applying a digital differentiator to the ramp, with appropriate checks and scaling, refer to Fig. 3(E). This turns the sawtooth input into a continuous function that can be differentiated, which allows the output signal to be processed through rate limits and output smoothing, in Fig. 3(E), (F) and (G).

(F) ROCOF Limits: Limits, set to measured frequency ± 0.5 Hz are derived from the final output signal, F_meas, and are applied to f_Hz, refer to Fig. 3(F). These limit values are coordinated with the bandwidth of the final filter stages to produce a measurement with ROCOF capability of ± 5 Hz/s.

(G) *Moving Average Filter*: The capped f_Hz signal is smoothed by a one cycle Moving Average Filter (MAF), primarily to smooth the input signal before passing to the integrator, refer to Fig. 3(G). The MAF maintains an integer number of samples per cycle by synchronising its sampling frequency with the measured frequency. A ten tap MAF is shown here but in practice > 100 taps are preferable. The MAF output feeds a first-order lag block whose output is frozen for pps voltage magnitudes below 0.1 pu

A. CALCULATED DESIGN CONSIDERATIONS FOR INTEGRATOR AND HYSTERESIS BLOCK

As previously mentioned, the control system parameters have been selected to track a ROCOF of up to ± 5 Hz/s. Equation (1) can be used to determine an appropriate integrator time constant, T_i, to provide sufficient output smoothing. Using the values from Table 1 in (1) we can calculate an

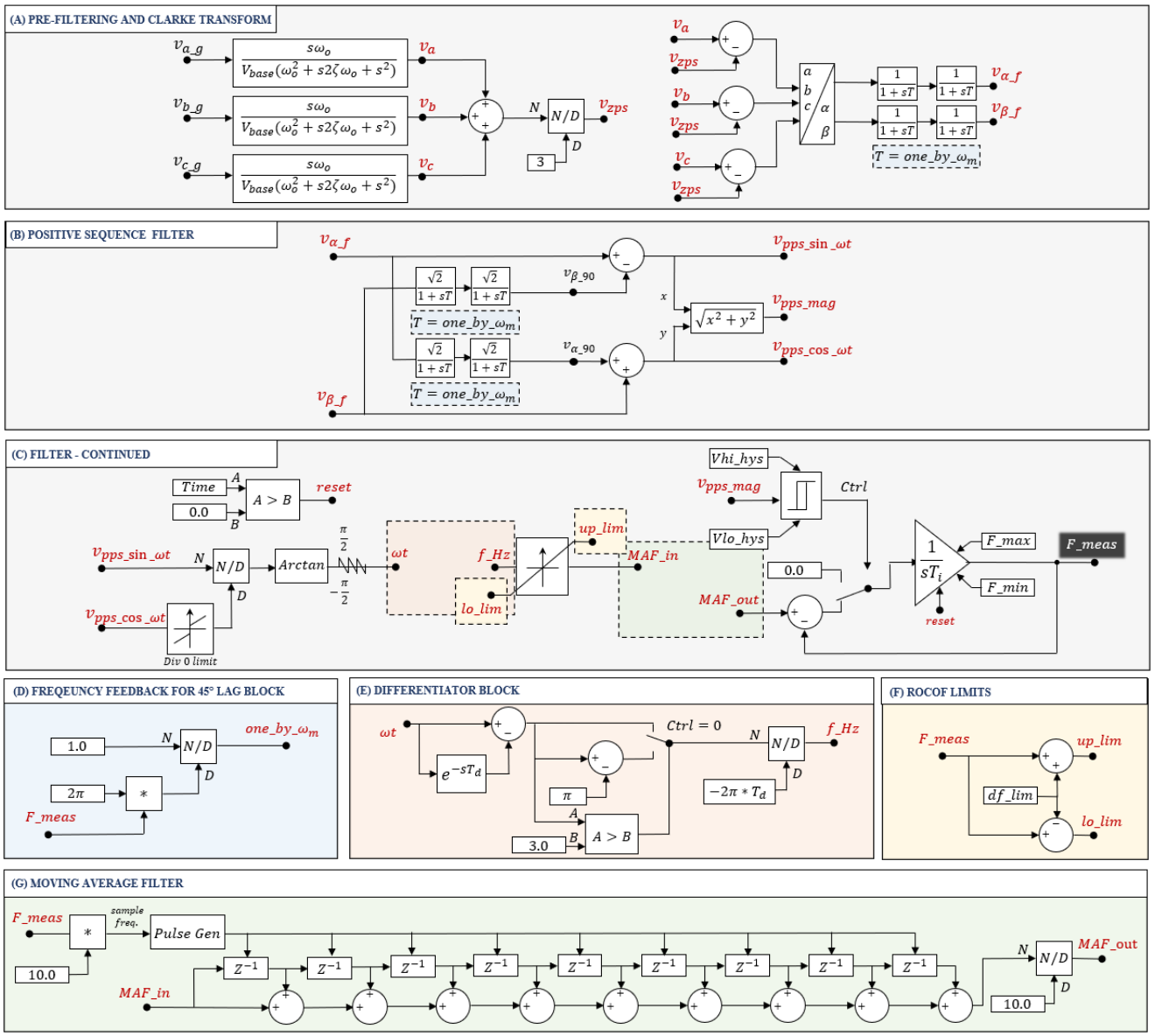

FIGURE 3. **Detailed block diagram for the PSP method.**

integrator time constant of 80 ms.

$$T_i = \frac{df\_lim}{(df/dt\_max)} - T_f \tag{1}$$

A common challenge arises for practical implementation of many control systems when measured input values are very close to 0. For frequency measurement, if voltage waveform magnitude approaches 0 pu, VT measurement accuracy becomes a critical factor. Hence, attempting to accurately measure voltage below 5% nominal is difficult [25], [26], [27]. To provide robustness to the PSP measurement algorithm, a lower threshold must therefore be set. To avoid single input switching logic, a hysteresis block has been selected to force the input to the integrator to be 0 whenever a voltage less than 0.05 pu is measured, which avoids the PSP method attempting to track frequency when no voltages are present. This threshold was chosen after appropriate testing demonstrated that frequency could be reliably tracked even with voltage magnitude as low as 0.05 pu.

IV. PERFORMANCE OF THE POSITIVE SEQUENCE PHASOR MEASUREMENT METHOD

To demonstrate the capability of the described PSP method, we present three sets of system studies: (A) SMIB type test studies with frequency ramps and network faults (Figs. 5 and 6), (B) playback of a real fault event and comparison to real PMU measurements (Figs. 7, 8(a-d)), and (C) an onerous SMIB study comparing the PSP method to the classic FFT, PLL and ZCD methods (Fig. 10).

Each test was constructed in PSCAD™, an electromagnetic transient (EMT) simulation environment. EMT simulation is required because instantaneous voltage

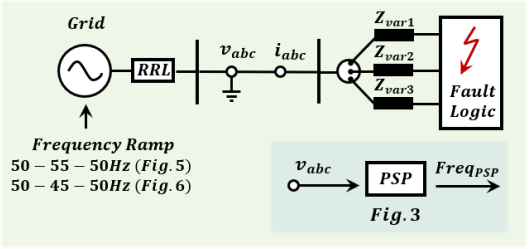

FIGURE 4. SMIB representation of the type test environment use to evaluate the PSP method.

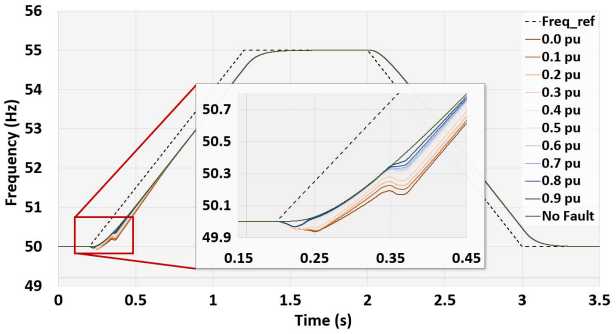

FIGURE 5. Frequency ramps ± 5 Hz/s (50-55-50 Hz); DLG fault applied at 200ms, with 120ms fault duration.

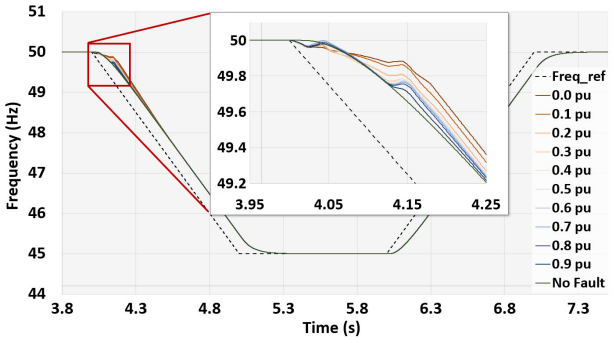

FIGURE 6. Frequency ramps ± 5 Hz/s (50-45-50 Hz); DLG fault applied at 4s, with 120ms fault duration.

waveforms are required by frequency measurement methods. The FWAV22 frequency measurement block, available from the standard components in the PSCAD™ library [28], was used for comparison purposes. This block employs a form of ZCD for its frequency measurement. Furthermore, the standard Phase Locked Loop (PLL) component [29] was used for the PLL method. The On-line Frequency Scanner (FFT) component [30] was used to demonstrate measurement via the FFT method.

A. TYPE TESTS FOR THE POSITIVE SEQUENCE PHASOR METHOD

To perform type tests a SMIB environment was created, represented in Fig. 4. This approach allows for a controlled frequency ramp to be applied to the RRL voltage source (RRL being shorthand for a Resistor-Resistor//Inductor source impedance – a common representation of voltage source impedance for simulation purposes). At the initiation of a frequency ramp (increase or decrease), a fault can be applied to onerously test the performance of the proposed PSP method, alongside existing methods. Various fault types can be readily applied, and source impedances can be varied to reflect weaker or stronger systems.

Type tests were first performed to determine the response to frequency ramps and faults simultaneously. Benchmarking for frequency ramps of ± 1, 2, 3, 4 and 5 Hz/s were undertaken. The maximum deviation between frequency reference (Freq_ref) and measurement when no fault was applied are; 0.085 Hz (± 1 Hz/s), 0.171 Hz (± 2 Hz/s), 0.256 Hz (± 3 Hz/s), 0.341 Hz (± 4 Hz/s), and 0.478 Hz (± 5 Hz/s).

Of the four fault types tested, single line-to-ground (SLG), double line-to-ground (DLG), three line-to-ground (3LG) and line-to-line (L-L), a 3LG fault, although onerous for the power system, is less difficult to track for the PSP method as the phase voltages are balanced. The design limit for our PSP is a DLG fault and thus frequency measurements for this fault are shown in Figs. 5 and 6.

In Fig. 5, a ± 5 Hz/s over-frequency ramp is applied to the SMIB voltage source at 0.2s, at the same time a DLG fault is applied. The known frequency reference is overlaid with the PSP algorithm outputs from repeated simulations where the fault depth is varied from 0.9 to 0.0 pu. The maximum deviation from the frequency reference occurs in the bolted fault case (0.0 pu). In Fig. 6, a similar series of fault studies is simulated in the presence of a ± 5 Hz/s under-frequency event, and similar performance is observed.

A summary of the results is presented in Table 2 for all fault types, with maximum deviation of frequency from the frequency reference presented (including the inherent deviation from the frequency reference due to the integrator and pre-filtering).

B. PLAYBACK EVENT – 14th OCTOBER 2022

On the 14th October 2022, a series of severe faults occurred in the Tasmanian power system. The compounded frequency and voltage event provides an ideal case to test the performance of the PSP method and other industry standard frequency measurements, such as the ZCD, PLL and FFT. The range of PMU measurements captured during this event, at a substation close to the fault location, are found in Fig. 1.

The captured voltage waveforms recorded by one of TasNetworks' high speed incident recorders were played back using the PSCAD™ File Read block. These voltage waveform measurements were sampled at 6.4 kHz and provided as inputs to the PSP control blocks (Fig. 3(A)).

The same inputs were also provided to ZCD, PLL and FFT blocks, with outputs subsequently passed through identical ramp rate limiters and output smoothing as used for the PSP method, illustrated in Fig. 3(C), to ensure meaningful comparisons. With this approach, the proposed and existing algorithms are tested on an actual event, thus providing a rigorous test of their performance.

TABLE 2. Summary of frequency ramp results for all fault types, freq-ref tracking of ± 5 Hz/s.

	Maximum Deviation (Δf Hz)			
Faulted phase(s) (V pu)	SLG	L-L	DLG	3LG
0.0	0.601	0.669	0.681	1.082
0.1	0.590	0.661	0.652	0.724
0.2	0.577	0.651	0.627	0.700
0.3	0.562	0.633	0.596	0.652
0.4	0.547	0.612	0.556	0.611
0.5	0.532	0.590	0.538	0.566
0.6	0.519	0.566	0.528	0.536
0.7	0.508	0.540	0.516	0.516
0.8	0.491	0.521	0.504	0.502
0.9	0.478	0.507	0.478	0.478
No Fault	0.478	0.478	0.478	0.478

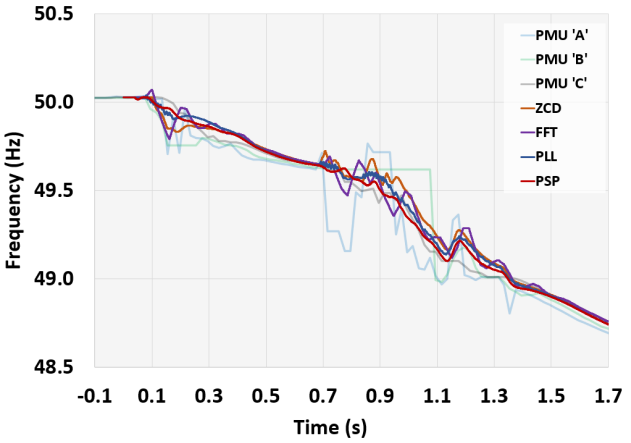

FIGURE 7. PMU frequency traces with various frequency measurement methods (including, PSP, PLL, ZCD and FFT), corresponding to the fault event in the Tasmanian power system on the 14th October 2022.

In Fig. 7 the PSP, ZCD, PLL and FFT derived measurements are overlaid against the data captured by the three PMUs, located at a nearby substation. To better highlight the performance of each method, Fig. 8(a-d) compares frequency calculated by each method in turn, against the PMU measurements. Fig. 8(a) illustrates how the PSP method robustly tracks frequency, even when the system is exposed to a series of deep faults which cause large variations in power system frequency. This result supports the supposition that PMU 'C' is apparently the only PMU which accurately tracks frequency. Both PMU 'C' and the PSP method appear to reliably produce the true underlying grid frequency.

In Fig. 8(b) the FFT method is shown to have measurement performance similar to that of PMUs 'A' and 'B', with measured values exhibiting the largest deviations in frequency with very high df/dt.

Frequency measured by the PLL method, illustrated in Fig. 8(c), can be seen generally to quite similar to the measurements of the PSP method, representing an improvement compared to the FFT method. However, in the presence of faults, the PLL cycles against the rate limits, resulting in rapid oscillations (inset of Fig. 8(c)). The combination of frequency and voltage disturbances, resulting from severe faults, is challenging even for established frequency measurement approaches such as the PLL method.

Lastly, we present the ZCD method in Fig. 8(d). The measurement performance of the ZCD method is similar to that of the FFT method. In the absence of faults, it is capable of adequately tracking frequency, following a similar trajectory as the measurement of PMU 'C'. However, the exposure to non-sinusoidal voltages and dc offsets during faults exposes the downsides of this method, with the method producing several abrupt changes in output which likely indicate inability to accurately track true underlying frequency during such transients.

These performance comparisons, using playback of real-world fault conditions, highlight two key challenges. Firstly, accurate tracking of frequency during complex transient conditions is challenging and requires robust assessment of measurement method performance. It is often not possible to know the exact underlying grid frequency, and thus judgement on whether measured values reflect realistic behavior, based on knowledge of the physical system, can be used to assess relative performance of measurements. Furthermore, critical frequency protection, such as under-frequency load shedding, requires accurate tracking of frequency; without a common synchronous source to provide a local reference, it is critical to be able to rely on VT measurements that reflect the underlying frequency.

Secondly, owing to the fact that the true underlying grid frequency itself can be difficult to ascertain during such transient conditions, assessment and comparison of real-world measurements should also be complemented with detailed EMT modelling and simulations of complex fault conditions. This is the focus of the following section.

C. SMIB COMPARISON – PSP, ZCD, FFT AND PLL METHOD

For further comparison and assessment of the proposed and existing frequency measurement methods, a basic SMIB environment is used, as per Fig. 9. Using this benchmarking approach, the same series of faults can be applied simultaneously to all four methods, providing an identical input for processing and performance. Since an RRL voltage source with fixed source frequency is used for these tests, any frequency deviation observed during transient fault conditions will be an artefact of poor frequency measurement, as a direct result of the algorithms employed. Using this approach, the PSP method is compared against the ZCD, FFT and PLL methods.

At a simulation time of 0.2 s an A-B line fault is applied, and at 0.22 s a B-C line fault is applied. Both are released after 0.12 s, to maintain their status as a credible fault in the Australian NEM. Frequency, which is set by the SMIB source,

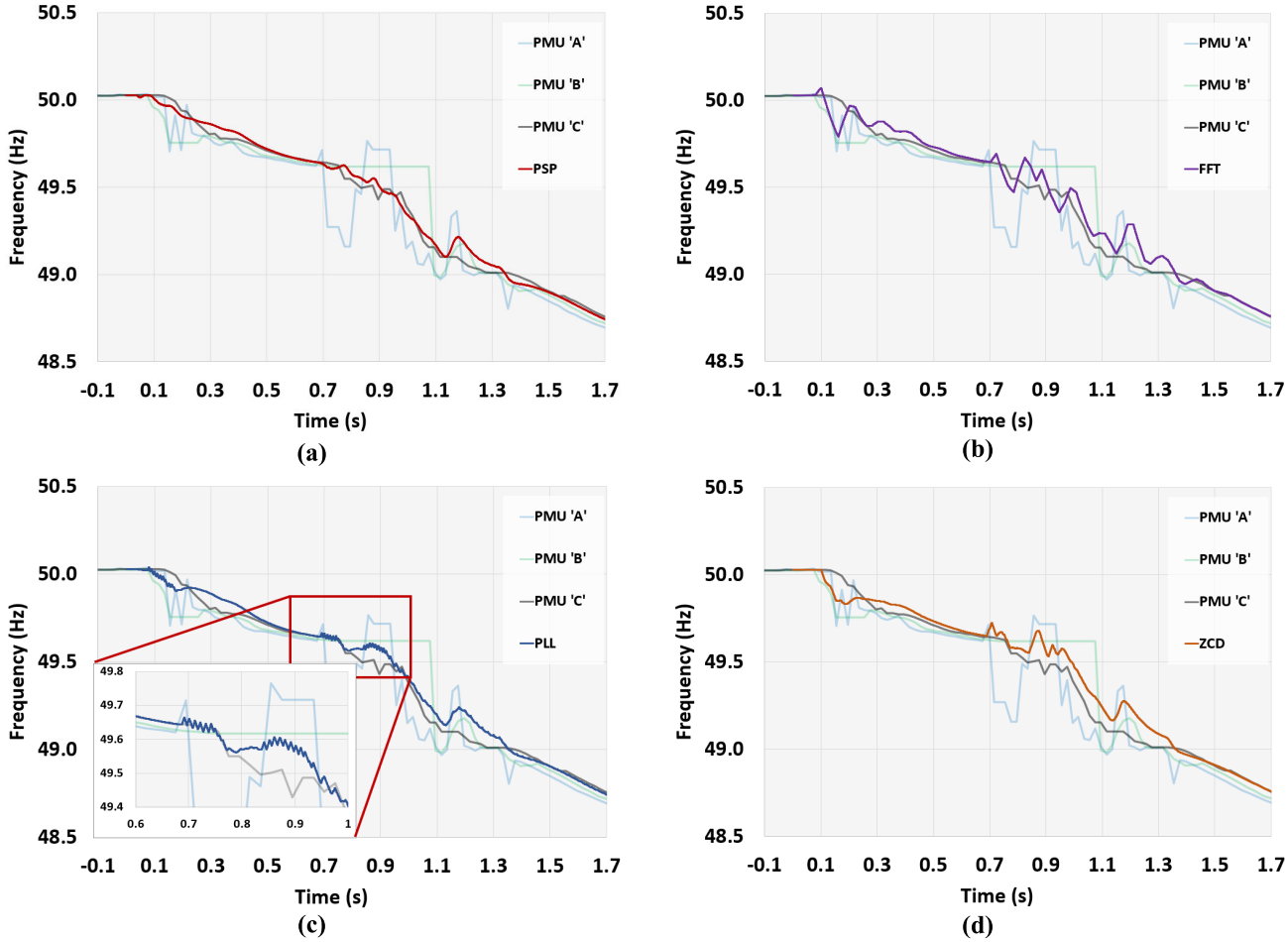

FIGURE 8. PMU frequency traces with: (a) PSP method (red trace), (b) FFT method (purple trace), (c) PLL method (blue trace), and (d) ZCD method (orange trace), corresponding to the fault event in the Tasmanian power system on the 14th October 2022.

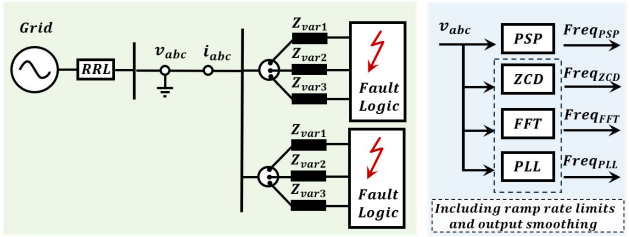

FIGURE 9. SMIB representation of the fault logic, ramp rate limits and output smoothing for PSP, ZCD, FFT and PLL methods.

is maintained at 50 Hz throughout. The resultant three-phase voltage waveforms, which each measurement method sees as input, are shown in Fig. 10(b), while the frequency measurements produced by each of the four methods are shown in Fig. 10(a).

The PSP method (red trace) limits the deviation of frequency and maintains the output to < 70 mHz error. In contrast, the ZCD, FFT and PLL methods (orange, purple and blue traces respectively) fail to accurately track frequency, since they are exposed to asymmetrical zero crossings and non-sinusoidal waveforms during fault inception and release. This clearly highlights the limitations of existing methods in

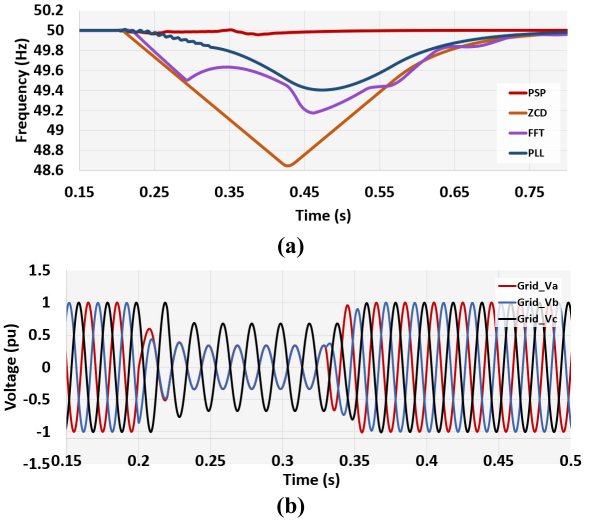

FIGURE 10. SMIB results: (a) frequency measured via both ZCD, FFT, PLL and PSP methods, and (b) three phase voltages during unbalanced faults (A-B at 0.2s and B-C at 0.22s, both for 120ms fault duration).

the presence of unbalanced credible faults, even with post-processing (ramp rate limit and output smoothing with a first

order lag), while simultaneously highlighting the robustness of our proposed method.

V. CONCLUSION

This paper has presented a modern, accurate and fault-tolerant positive phase sequence method for grid frequency measurement. This method is straightforward to implement and is suitable for use by power system operators or for automatic control of IBR if reliable fast frequency response is required. A complete set of control block diagrams has been presented, to facilitate integration into modelling packages, phasor measurement units or other hardware devices requiring robust frequency measurement. To demonstrate the measurement method's performance, algorithm testing under a range of rapidly changing frequency and voltage conditions has been conducted. Comparison with real PMU measurements in a power system during a major fault event has revealed equivalent or considerably improved performance than currently deployed devices. Furthermore, the method has been benchmarked against the common ZCD, FFT, PLL measurement methods, using identical filtering, and has been shown to provide far superior measurement accuracy. The method described in this paper provides a means for IBR to reliably participate in new fast frequency markets such as the new R1 FCAS market in Australia, whilst also enabling further applications for power systems globally. The details provided allow this method to be readily implemented and deployed by manufacturers and designers of frequency measuring equipment, thus facilitating accurate primary frequency measurement across the power industry as networks worldwide shift to higher penetrations of IBR.

ACKNOWLEDGMENT

The authors are grateful for the support and encouragement given by the directors and management of Tasmanian Networks Pty. Ltd., (TasNetworks) in the production of this article.

REFERENCES

[1] L. Zhan, B. Xiao, F. Li, and Y. Liu. (Sep. 1, 2021). *Open Source Fault-tolerant Grid Frequency Measurement for Solar Inverters*. Accessed: Dec. 2023. [Online]. Available: https://www.osti.gov/biblio/1823357

[2] K. Prabakar et al., "Understanding impacts of frequency calculations on underfrequency load shedding," in *Proc. IEEE Rural Electr. Power Conf. (REPC)*, Cleveland, OH, USA, Apr. 2023, pp. 39–43, doi: 10.1109/repc49397.2023.00015.

[3] R. Luhtala, H. Alenius, T. Messo, and T. Roinila, "Online frequency response measurements of grid-connected systems in presence of grid harmonics and unbalance," *IEEE Trans. Power Electron.*, vol. 35, no. 4, pp. 3343–3347, Apr. 2020, doi: 10.1109/TPEL.2019.2943711.

[4] AEMO. (Jul. 2023). *Market Ancillary Service Specification*. Accessed: Oct. 15, 2023. [Online]. Available: https://aemo.com.au/en/energy-systems/electricity/national-electricity-market-nem/system-operations/ancillary-services/market-ancillary-services-specification-and-fcas-verification-tool

[5] G. Rietveld, P. S. Wright, and A. J. Roscoe, "Reliable rate-of-change-of-frequency measurements: Use cases and test conditions," *IEEE Trans. Instrum. Meas.*, vol. 69, no. 9, pp. 6657–6666, Sep. 2020, doi: 10.1109/TIM.2020.2986069.

[6] Z. Peng, Q. Peng, Y. Zhang, H. Han, Y. Yin, and T. Liu, "Online inertia allocation for grid-connected renewable energy systems based on generic ASF model under frequency nadir constraint," *IEEE Trans. Power Syst.*, vol. 39, no. 1, pp. 1615–1627, Jan. 2023, doi: 10.1109/TPWRS.2023.3267267.

[7] H. Yin et al., "Field measurement and analysis of frequency and RoCoF for low-inertia power systems," *IEEE Trans. Ind. Electron.*, vol. 71, no. 7, pp. 7996–8006, Jul. 2024, doi: 10.1109/TIE.2023.3303622.

[8] M. G. Arcia, Z. G. Sanchez, H. H. Herrera, J. A. G. C. Cruz, J. I. S. Ortega, and G. C. Sánchez, "Frequency response analysis under faults in weak power systems," *Int. J. Electr. Comput. Eng.*, vol. 12, no. 2, p. 1077, Apr. 2022, doi: 10.11591/ijece.v12i2.pp1077-1088.

[9] J. Ting, B. Wang, R. W. Kenyon, and A. Hoke, "Evaluating methods for measuring grid frequency in low-inertia power systems," in *Proc. IEEE Kansas Power Energy Conf. (KPEC)*, Manhattan, KS, USA, Apr. 2022, pp. 1–6, doi: 10.1109/KPEC54747.2022.9814727.

[10] M. Davies, J. Paoli, and C. Wembridge, "Benefits in harnessing the latent reactive current injection capability of inverter-based resources in the Australian power system," in *Proc. CIGRE Int. Symp.*, Cairns, QLD, Australia, Sep. 2023, Paper 1238.

[11] H. Yin et al., "Precise ROCOF estimation algorithm for low inertia power grids," *Electric Power Syst. Res.*, vol. 209, Aug. 2022, Art. no. 107968, doi: 10.1016/j.epsr.2022.107968.

[12] L. Zhan et al., "Fault-tolerant grid frequency measurement algorithm during transients," *IET Energy Syst. Integr.*, vol. 2, no. 3, pp. 173–178, Sep. 2020, doi: 10.1049/iet-esi.2019.0126.

[13] J. Li, Z. Teng, Y. Wang, S. You, Y. Liu, and W. Yao, "A fast power grid frequency estimation approach using frequency-shift filtering," *IEEE Trans. Power Syst.*, vol. 34, no. 3, pp. 2461–2464, May 2019, doi: 10.1109/TPWRS.2019.2892599.

[14] K. Tuttelberg, J. Kilter, D. Wilson, and K. Uhlen, "Estimation of power system inertia from ambient wide area measurements," *IEEE Trans. Power Syst.*, vol. 33, no. 6, pp. 7249–7257, Nov. 2018, doi: 10.1109/TPWRS.2018.2843381.

[15] Y. Mitsugi, H. Hashiguchi, T. Shigemasa, Y. Ota, T. Terazono, and T. Nakajima, "Control hardware-in-the-loop simulation on fast frequency response of battery energy storage system equipped with advanced frequency detection algorithm," *IEEE Trans. Ind. Appl.*, vol. 57, no. 6, pp. 5541–5551, Nov. 2021, doi: 10.1109/TIA.2021.3107223.

[16] L. Zhan, Y. Liu, and Y. Liu, "A Clarke transformation-based DFT phasor and frequency algorithm for wide frequency range," *IEEE Trans. Smart Grid*, vol. 9, no. 1, pp. 67–77, Jan. 2018, doi: 10.1109/TSG.2016.2544947.

[17] T. Bains, I. Voloh, V. Chakrapani, and C. Mistry, "Frequency measurement in protective relays and impact by renewable energy sources," in *Proc. CIGRE Int. Symp.*, Cairns, QLD, Australia, Sep. 2023, Paper 1405.

[18] M. M. Begovic, P. M. Djuric, S. Dunlap, and A. G. Phadke, "Frequency tracking in power networks in the presence of harmonics," *IEEE Trans. Power Del.*, vol. 8, no. 2, pp. 480–486, Apr. 1993, doi: 10.1109/61.216849.

[19] C. Wembridge, M. Davies, E. Franklin, S. Lyden, and M. Negnevitsky, "Dynamic voltage support of six-pulse bridge inverters: Equitable performance specification for future grids," in *Proc. IEEE Int. Conf. Energy Technol. Future Grids (ETFG)*, Wollongong, NSW, Australia, Dec. 2023, pp. 1–6.

[20] P. S. Wright, P. N. Davis, K. Johnstone, G. Rietveld, and A. J. Roscoe, "Field measurement of frequency and ROCOF in the presence of phase steps," *IEEE Trans. Instrum. Meas.*, vol. 68, no. 6, pp. 1688–1695, Jun. 2019, doi: 10.1109/TIM.2018.2882907.

[21] A. G. Phadke, J. S. Thorp, and M. G. Adamiak, "A new measurement technique for tracking voltage phasors, local system frequency, and rate of change of frequency," *IEEE Power Eng. Rev.*, vol. PER-3, no. 5, pp. 23–23, May 1983, doi: 10.1109/MPER.1983.5519136.

[22] AEMO. (Oct. 2022). *Incident Report—Trip of Liapootah—Palmerston—Waddamana 220 KV Lines*. Accessed: Oct. 15, 2023. [Online]. Available: https://aemo.com.au/-/media/files/electricity/nem/market_notices_and_events/power_system_incident_reports/2022/trip-of-liapootah—palmerston—waddamana-no-1-and-no-2-220-kv-lines.pdf?la=en

[23] *IEEE Standard for Interconnection and Interoperability of Inverter-Based Resources (IBRs) Interconnecting With Associated Transmission Electric Power Systems*, IEEE IEEE Standard 2800-2022, Apr. 2800, pp. 1–180, doi: 10.1109/IEEESTD.2022.9762253.

[24] E. Clarke, C. N. Weygandt, and C. Concordia, "Overvoltages caused by unbalanced short circuits effect of amortisseur windings," *Trans. Amer. Inst. Electr. Engineers*, vol. 57, no. 8, pp. 453–468, Aug. 1938, doi: 10.1109/T-AIEE.1938.5057833.
[25] D. Gallo, C. Landi, M. Luiso, P. Tosato, D. Macii, and D. Brunelli, "A testbed for the experimental characterization of estimation algorithms for phasor measurement units," in *Proc. IEEE Int. Workshop Appl. Meas. Power Syst. (AMPS)*, Liverpool, U.K., Sep. 2017, pp. 1–6, doi: 10.1109/AMPS.2017.8078341.
[26] P. Castello, C. Muscas, P. A. Pegoraro, S. Sulis, and S. Toscani, "Experimental characterization of dynamic methods for synchrophasor measurements," in *Proc. IEEE Int. Workshop Appl. Meas. Power Syst. (AMPS)*, Aachen, Germany, Sep. 2014, pp. 1–6, doi: 10.1109/AMPS.2014.6947709.
[27] M. S. Sachdev et al. (2004). *Understanding Microprocessor-based Technology Applied to Relaying*. Accessed: May 8, 2024. [Online]. Available: https://www.pes-psrc.org/kb/report/037.pdf
[28] PSCAD. (May 2024). *FWAV22 Frequency/RMS/Phase Meter Component*. Accessed: May 8, 2024. [Online]. Available: https://www.pscad.com/webhelp/EMTDC_Tools_Library/Meters/fwav22.htm
[29] PSCAD. (May 2024). *Phase Locked Loop (PLL) Component*. Accessed: May 8, 2024. [Online]. Available: https://www.pscad.com/knowledgebase/topic-448/v-
[30] PSCAD. (May 2024). *On-Line Frequency Scanner (FFT) Component*. Accessed: May 8, 2024. [Online]. Available: https://www.pscad.com/webhelp/Master_Library_Models/CSMF/On-Line_Frequency_Scanning/fft.htm

CHRIS WEMBRIDGE (Member, IEEE) was born Victoria, Australia, in 1992. He received the B.Eng. degree (Hons.) in electrical/electronic engineering from Deakin University, Geelong, Victoria, in 2015. He is currently pursuing the Ph.D. degree with the University of Tasmania. He has been a Senior Network Performance Engineer with TasNetworks, Hobart, Tasmania, Australia, since 2021. His research interests include machine theory, protection of power systems, power electronic systems, and the grid integration of renewable energy resources. He is a Chartered Professional Engineer of Engineers Australia; and a member of the Institution of Engineering and Technology (IET), CIGRE, and the Electric Energy Society of Australia.

MARK DAVIES was born Birmingham, U.K., in 1963. He received the B.Sc. (Comm.) degree in electrical/electronic engineering and the Ph.D. degree in control systems for static var compensators from Staffordshire University, U.K., in 1985 and 1997, respectively. He was with GEC, U.K., from 1981 to 2000; and Siemens, USA/Germany, from 2000 to 2011. He has been with TasNetworks, Hobart, Tasmania, Australia, since 2011. He has contributed in the field of power electronics and power system simulation being a Key Design Engineer of the world's first multilevel converters for both STATCOM and HVDC applications. Since 2011, he has been on the operation of Tasmanian power networks, especially on the integration of new connections. He is a member of CIGRE and the Electric Energy Society of Australia.

JAMES LORD was born Tasmania, Australia, in 1991. He received the B.Eng. degree (Hons.) in electrical power engineering from the University of Tasmania, Hobart, Tasmania, in 2013. Since 2014, he has been with TasNetworks, Hobart, as a Graduate Engineer, a Metering and Protection Engineer, a Network Performance Engineer, and a Senior Network Performance Engineer. His work has focused on the connection of renewable generation to the Tasmanian transmission networks. He is a member of CIGRE.

EVAN FRANKLIN (Member, IEEE) was born Tasmania, Australia, in 1976. He received the B.Eng. degree (Hons.) in electrical engineering from the University of Tasmania, Hobart, Tasmania, in 1996, and the Ph.D. degree from The Australian National University, Australia, in 2006. He is currently an Associate Professor of energy and power systems with the University of Tasmania. His research interests include the integration of renewable energy generation into distribution networks and power systems and the role of energy storage in future energy systems. He is a member of CIGRE and Engineers Australia.

SARAH LYDEN (Member, IEEE) was born Tasmania, Australia, in 1988. She received the combined B.Sc. and B.Eng. degree (Hons.) in mathematics and mechatronics and the Ph.D. degree from the University of Tasmania, Hobart, Tasmania, in 2011 and 2015, respectively. She is currently a Senior Lecturer with the University of Tasmania. Her research interests include control and grid integration of renewable energy sources, microgrid systems, and engineering education. She is a Chartered Professional Engineer and a member of Engineers Australia and the Electric Energy Society of Australia.

MICHAEL NEGNEVITSKY (Fellow, IEEE) received the B.S.E.E. (Hons.) and Ph.D. degrees from the Byelorussian University of Technology, Minsk, Belarus, in 1978 and 1983, respectively. He is the Chair Professor of power engineering and computational intelligence and the Director of the Centre for Renewable Energy and Power Systems, University of Tasmania, Hobart, Tasmania, Australia. His research interests include power system analysis, power economics, microgrids and smart grids, and intelligent systems applications in power systems. He is a Chartered Professional Engineer and a fellow of Engineers Australia.